



OPEN

Crystal orientation of epitaxial film deposited on silicon surface

Satoru Kaneko^{1,8}✉, Takashi Tokumasu², Manabu Yasui¹, Masahito Kurouchi¹, Daishi Shiojiri¹, Shigeo Yasuhara³, Sumanta Kumar Sahoo⁴, Musa Mutlu Can⁵, Rwei Sung Yu⁶, Kripasindhu Sardar⁷, Masahiro Yoshimura⁷, Masaki Azuma^{1,8}, Akifumi Matsuda⁸ & Mamoru Yoshimoto⁸

Direct growth of oxide film on silicon is usually prevented by extensive diffusion or chemical reaction between silicon (Si) and oxide materials. Thermodynamic stability of binary oxides is comprehensively investigated on Si substrates and shows possibility of chemical reaction of oxide materials on Si surface. However, the thermodynamic stability does not include any crystallographic factors, which is required for epitaxial growth. Adsorption energy evaluated by total energy estimated with the density functional theory predicted the orientation of epitaxial film growth on Si surface. For lower computing cost, the adsorption energy was estimated without any structural optimization (simple total of energy method). Although the adsorption energies were different on simple ToE method, the crystal orientation of epitaxial growth showed the same direction with/without the structural optimization. The results were agreed with previous simulations including structural optimization. Magnesium oxide (MgO), as example of epitaxial film, was experimentally deposited on Si substrates and compared with the results from the adsorption evaluation. X-ray diffraction showed cubic on cubic growth [MgO(100)//Si(100) and MgO(001)//Si(001)] which agreed with the results of the adsorption energy.

Direct growth of oxide film on silicon surface has been explored to combine silicon technology and functioning oxide materials for device applications^{1–9}. However silicon surface can be easily oxidized in oxygen atmosphere before oxide film deposition. And interdiffusion or chemical reaction between silicon and those oxide materials prevent direct growth of oxide film on silicon surface. In general, a buffer layer is required between oxide and silicon surface for epitaxial growth^{10–14}. For selection of oxide materials expected to grow on silicon surface, Schlom et al. reported thermodynamic stability of binary oxides in contact with silicon surface¹⁵, and comprehensively investigate the thermodynamic stability of more than 80 binary oxides. However, the thermodynamic stability is not concerned with any information about crystallography such as orientation of epitaxial film growth.

In order to evaluate the crystallographic stability, an adsorption energy was estimated on target materials. Magnesium oxide (MgO), for an example, was placed on silicon (Si) surface (supercell) as shown in Fig. 1 and the total energy was calculated by using molecular dynamics, and the crystal orientation of epitaxial growth was evaluated by the adsorption energy¹⁶. In previous study, carbon clusters were also placed on a variety of substrates, and the adsorption energy was used to select an appropriate substrate for graphene growth, and *super flat* graphene^{17,18} was verified on the candidate target. For graphene growth, carbon clusters were also optimized as well as optimizing substrate surface before constructing supercells, and position and orientation of clusters were also optimized during the calculation.

Optimization of substrate surface and cluster migration requires time-cost and resources. Although an accurate calculation is available with time consuming and expense, rough estimations can be enough for many cases. In this study, stability of crystal orientation of MgO film was evaluated on Si surface. Many study has been explored on epitaxial MgO on Si substrate^{2–4,6–8,19–26}, however some difficulty still remain on the topic. In addition to aforementioned thermal stability, the difficulty of epitaxial growth comes from large lattice mismatch and narrow deposition conditions²⁷, and post-annealing or buffer layer might be required¹³. The lattice constants, for example, of MgO is 4.21 and whereas that of Si is 5.431 Å, implying a mismatch of 22%, which can be more than enough reason to exclude MgO from candidate materials deposited on Si substrate. However, epitaxial growth of MgO has been reported on Si(001) substrates^{3,4,7,8}.

In general, MgO can epitaxially grow on Si(001) substrate with the relation of cubic on cubic growth [MgO(001) // Si(001) and MgO(100) // Si(100)] or 45° rotation growth [MgO(001) // Si(001) and MgO(110) //

¹Kanagawa Institute of Industrial Science and Technology (KISTEC), Ebina, Kanagawa 243-0435, Japan. ²Tohoku University, Sendai, Miyagi 980-8577, Japan. ³Japan Advanced Chemicals, Sagami-hara, Kanagawa 252-0243, Japan. ⁴Radhakrishna Institute of Technology and Engineering, Bhubaneswar, Odisha 752057, India. ⁵Istanbul University, Istanbul 34134, Turkey. ⁶Asia University, Taichung 41354, Taiwan. ⁷National Cheng Kung University, Tainan 701, Taiwan. ⁸Tokyo Institute of Technology, Yokohama 226-8502, Japan. ✉email: satoru@kistec.jp

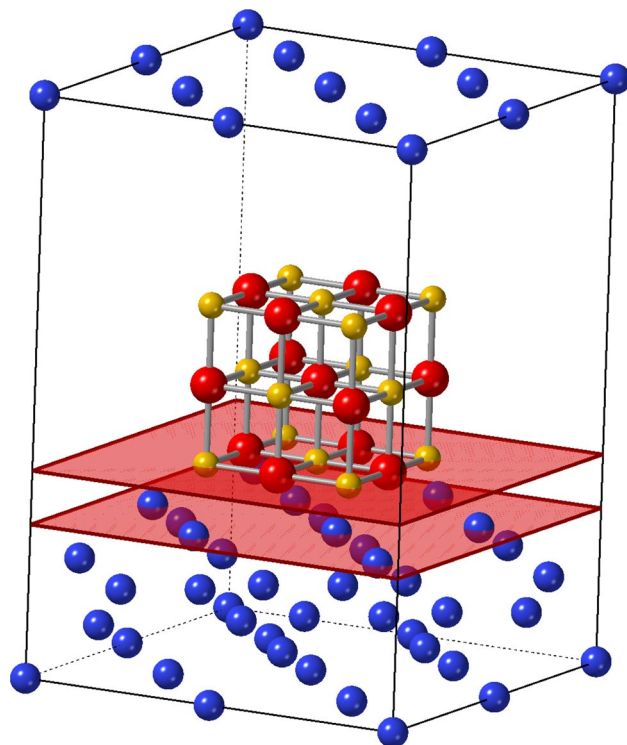


Figure 1. Schematics of supercell consisting MgO cluster placed on silicon surface with varied distances. The red flat planes show the surface of Si substrate and the bottom of MgO cluster.

Si(100)], as shown in Fig. 2. In order to predict the orientation of crystal growth, it must be sufficient to compare the adsorption energy between cubic growth and 45° growth. The adsorption energy was evaluated with total energy (E_{tot}) of oxide cluster, substrate surface and supercell consisting of the cluster and surface. For low cost computing, the simulation can exclude optimization of substrate surface and cluster migration. Computing cost can be tremendously reduced without those optimizations by using molecular dynamics in the supercell. MgO cluster was simply placed on Si(001) with relation of cubic or 45° arrangements, and the adsorption energy was estimated without the optimization of surface structure nor cluster migration. In this study, we introduce a simple method to evaluate adsorption energy by simple total of energies method (simple ToE method).

MgO films were experimentally deposited on Si substrate by a pulsed laser deposition (PLD) and examined by variety of X-ray diffraction (XRD) methods, ordinal θ - 2θ scan, in-plane $\theta - 2\theta$ scan, ϕ scan, reciprocal space mapping and Pseudopowder XRD^{5,28}, and epitaxial growth of MgO was verified on the Si surface. Interestingly,

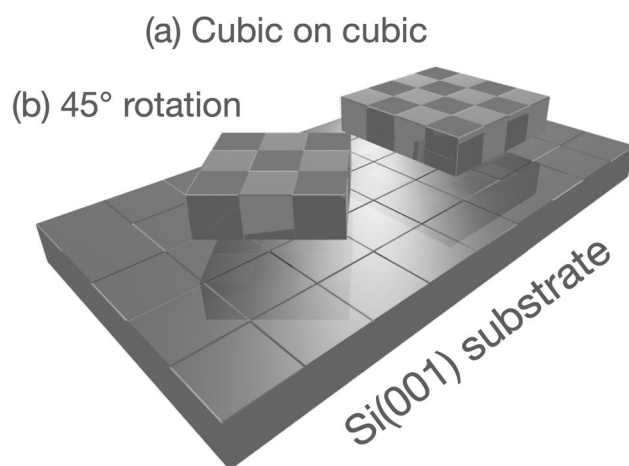


Figure 2. Schematics of growth of MgO deposited on Si substrate. MgO(001) cluster grows on Si(001) along with the relation of (a) cubic on cubic growth [$\text{MgO}(100) // \text{Si}(100)$] and (b) 45° rotation growth [$\text{MgO}(110) // \text{Si}(100)$].

construction of lattice constants is reported on MgO film deposited on Si(001), and under low vacuum atmosphere nano cubic MgO grows on Si surface²⁹. Density functional theory(DFT) calculation shows the construction can be caused on defect model of MgO structure²⁸, and improves the domain mismatch⁵.

Experimental methods

Convention cells of $2 \times 2 \times 2$ Si and $1 \times 1 \times 1$ MgO cluster were prepared, and vacuum slab of 1 nm, was inserted on $2 \times 2 \times 2$ Si surface. Supercell was generated by placing MgO cluster into the vacuum slab on Si surface with varied distances from the Si surface: red planes shown in Fig. 1. The arrangement between MgO and Si were MgO(100) // Si(100) (cubic growth) or MgO(110) // Si(100) (45° growth). Crystal structure was constructed by using the CrystalMaker X, and converted into appropriate format by using cif2cell³⁰.

For calculation of adsorption energy, as shown in Fig. 3, total energies of (a) MgO cluster, (b) Si(001) with vacuum slab and (c) supercell of MgO inserted into vacuum slab were calculated by using the ABINIT code³¹, a project of the Louvain, based on density functional theory. A parallel version of ABINIT was prepared with openmpi and performed on Intel Zeon and Apple M1. The projector augmented wave method (PAW)³² was used with the LDA atomic datasets on the ABINIT web site (<https://www.abinit.org/psp-tables>). The energy difference for self-consistent field was set at 1.0×10^{-6} Hartree (Ha) with energy cut-off of 40 Ha and paw energy cut-off of 60 Ha.

Pulsed laser deposition (PLD) was a versatile method and simple compared to another method like a molecular beam epitaxy³³ and used for depositing various films^{34–36} including nano particles^{37,38}. Film deposition was performed by the PLD using a slower Q-switched YAG laser³⁹ with a fourth harmonics of 266 nm at the repetition rate of 2 Hz, and sputtering method was also employed to deposit MgO film on Si(001) substrates. X-ray diffraction was employed to verify the epitaxial growth, in-plane crystal orientation, and film thickness.

Results and discussion

In spite of large lattice mismatch ($\sim 22\%$), MgO thin film was well known grown epitaxially on Si substrates^{1,6,7}. Although 45° growth (9% mismatch) is preferable than cubic on cubic growth (23%), with a concept of domain mismatch^{5,40,41}, cubic on cubic growth can be preferable. In the domain epitaxial growth⁴², m unit lattices of the film match with k of the Si substrate. The domain coherent strain is defined as with the lattice coherent strain as,

$$2 \frac{ma_{\text{MgO}} - ka_{\text{Si}}}{ma_{\text{MgO}} + ka_{\text{Si}}},$$

instead of ordinal lattice mismatch as,

$$2 \frac{a_{\text{MgO}} - a_{\text{Si}}}{a_{\text{MgO}} + a_{\text{Si}}}.$$

Either concept only includes crystallographic relations. Schlom et al. comprehensively investigate the thermodynamic stability of more than 80 binary oxides including MgO, however the thermodynamic stability does not include any factors related with the orientation of crystal growth.

In this study, adsorption energy was introduced to evaluate the crystal orientation of epitaxial growth. Adsorption energy was estimated from total energies of MgO cluster, Si surface, and supercell as,

$$E_{\text{ads}} = E_{\text{supercell}} - E_{\text{Si}} - E_{\text{MgO}},$$

where E_{ads} is an adsorption energy, and $E_{\text{supercell}}$, E_{Si} and E_{MgO} shows total energy of supercell, Si surface and MgO cluster, respectively, as shown in Fig. 3. Supercell was constructed by inserting MgO cluster on Si(001) surface with the relation of Mg atom placed on Si atom (Mg-centered) or O atom placed on Si atom (O-centered), and adsorption energy was estimated as shown in Fig. 4a,b. MgO clusters were placed on the Si surface with the distance from 0.14 to 0.25 nm.

The adsorption energy was stable on cubic growth with Mg-centered on Si atom. In the case of O atom placed on Si atom (O-centered), the adsorption energy was quite higher compared to Mg-centered with both cubic and

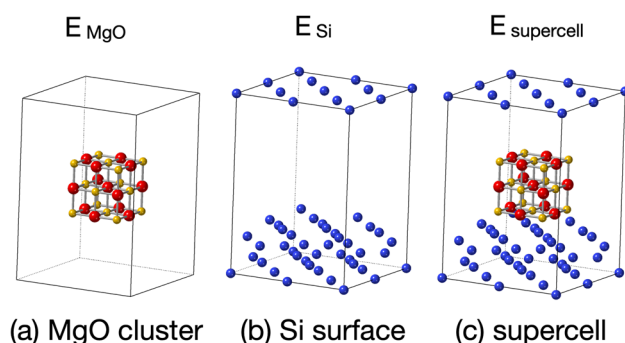


Figure 3. Adsorption energy, E_{ads} , was calculated by $E_{\text{abs}} = E_{\text{supercell}} - E_{\text{Si}} - E_{\text{MgO}}$.

45° growth. It might be related to the binding energy of atoms between Mg–Si and O–Si atoms. The cubic growth preferred to 45° growth agreed with our previous study using the Next-Generation Integrated Supercomputation System at Advanced Fluid Information Research Center, Institute of Fluid Science, Tohoku University. The calculation includes structural optimization and cluster migration together with optimization of supercell structure.

The calculation of the simple ToE method was usually less than 10 or 20 hours for the first time, and couple to several hours for following in chain the calculations in the multi-dataset mode of abinit code. The abinit code restarts calculation with wavefunction generated by previous calculation for speed up. While the calculations took more than 30 hours by the Supercomputation System at Advanced Fluid Information Research Center, the simple ToE method showed the same results less than half computing time on a Home PC, and dependent on convergence condition, the computing time was reduced by less than quarter compared to the calculation by Supercomputation System at Tohoku University. In order to evaluate the direction of crystal growth, precise calculation is not required for simulations.

MgO films were experimentally deposited on Si(001) substrates by a PLD system and sputtering methods. Figure 5 shows the in-plane $\theta - 2\theta$ XRD using Si(220) peak. MgO(220) peak was observed with Si(220) peaks, indicating MgO grew with relation of cubic on cubic growth [MgO(001) // Si(001) and MgO(110) // Si(110)]^{5,28}. X-ray reflectivity revealed the film thickness to be ~ 50 nm, and surface roughness of ~ 3 nm. The experimental results showed cubic growth, which agreed with the simulation used with the simple ToE method.

For lower computing cost, adsorption energy was evaluated without structural optimization (simple ToE method). Although adsorption energy were estimated to be different values, the adsorption energy showed the same trend on stability of MgO cluster on Si surface. The crystal growth of MgO showed the same direction on Si surface with/without structural optimization. The simple ToE method allows us to evaluate adsorption energy at relatively-low computing cost, and can be performed on home PC.

MgO thin films grew on Si(001) substrate with cubic on cubic growth, and the lattice constant is often contracted^{7,43–45}. The first principle theory shows the stability of the contracted structure with Schottky defect model, and the contracted structure result in better domain mismatch⁵. The advantage of cubic on cubic over 45° rotation growth is supported by (1) thermal stability between MgO and Si¹⁵, (2) domain epitaxy⁵, (3) the defect model, and (4) crystallographic stability (this work).

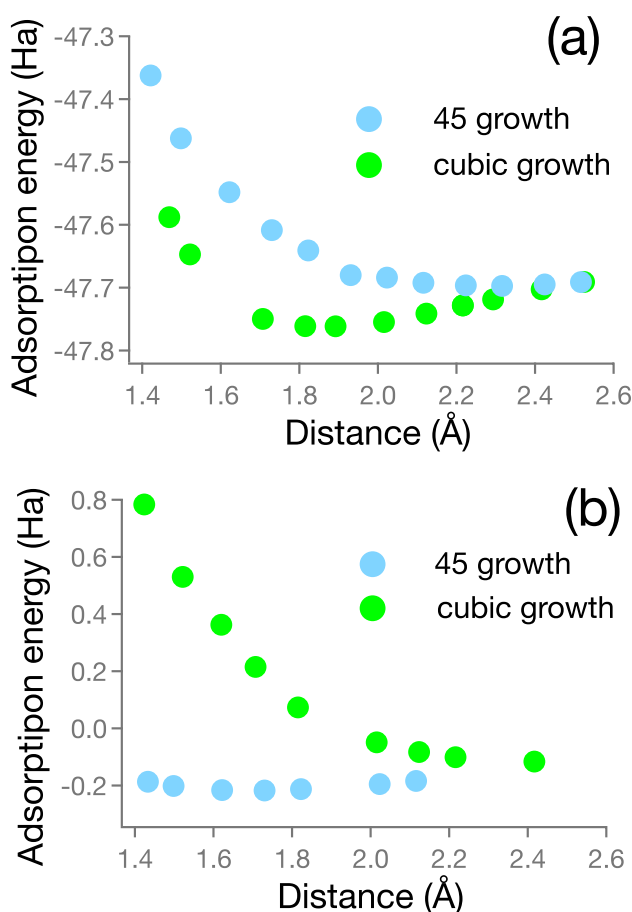


Figure 4. Adsorption energy estimated by simple total energy. (a) Mg atom and (b) O atom placed on Si atom.

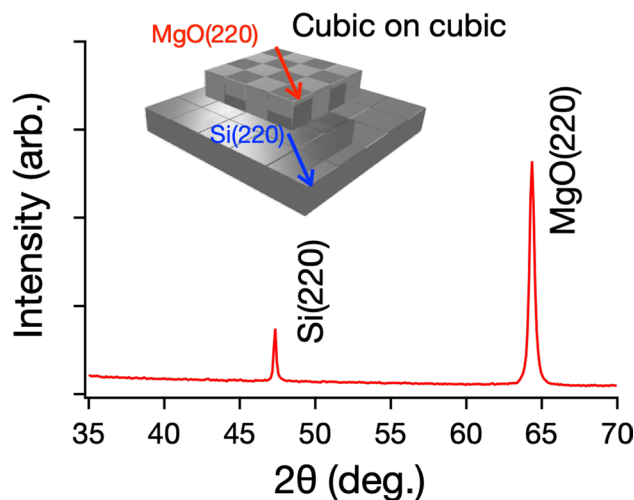


Figure 5. In-plane $\theta - 2\theta$ XRD of Si(220) peak together with MgO(220) peak, indicating cubic on cubic growth of MgO on Si substrate.

Summary

We proposed the simple ToE method to estimate an adsorption energy for prediction of crystal orientation of epitaxial growth on silicon substrate. The supercell constructed as target cluster inserted into vacuum slab on substrate surface without optimization for surface nor structural optimization. The total energy was simply calculated on the supercell without any optimization, and the absorption energy was estimated as the different energy of the supercells (as shown in Fig. 4). However, the simple method was sufficient for evaluation of the orientation of crystal growth, and computing time was less than half compared to previous report using supercomputer systems. This method is versatile method and can be performed on variety of combination of epitaxial growth.

Data availability

The datasets generated during and/or analysed during the current study are available from the corresponding author on reasonable request.

Received: 8 April 2024; Accepted: 7 May 2024

Published online: 13 May 2024

References

1. Fork, D. K., Fenner, D. B., Connell, G. A. N., Phillips, J. M. & Geballe, T. H. Epitaxial yttria-stabilized zirconia on hydrogen-terminated si by pulsed laser deposition. *Appl. Phys. Lett.* **57**, 1137 (1990).
2. Fork, D. K., Ponce, F. A., Tramontana, J. C. & Geballe, T. H. Epitaxial mgo on si(001) for y-ba-cu-o thin-film growth by pulsed laser deposition. *Appl. Phys. Lett.* **58**, 2294 (1991).
3. Kim, S. & Hishita, S. Growing batio₃ thin films on si(100) with mgo-buffer layers by sputtering. *Thin Solid Films* **281–282**, 449 (1996).
4. Kim, S. & Hishita, S. Preparation and characterization of batio₃ thin films on mgo-buffered si(100) substrates by rf sputtering. *J. Mater. Res.* **12**, 1152 (1997).
5. Kaneko, S., Funakubo, H., Kadowaki, T., Hirabayashi, Y. & Akiyama, K. Cubic-on-cubic growth of a mgo(001) thin film prepared on si(001) substrate at low ambient pressure by the sputtering method. *Europhys. Lett.* **81**, 46001 (2008).
6. Chen, T. I., Li, X. M., Zhang, S. & Zhang, X. Comparative study of epitaxial growth of pt and ir electrode films grown on mgo-buffered si(100) by pld. *Appl. Phys. A* **80**, 73 (2005).
7. Niu, F., Meier, A. L. & Wessels, B. W. Epitaxial growth and strain relaxation of mgo thin films on si grown by molecular beam epitaxy. *J. Vacuum Sci. Technol. B* **24**, 2586 (2006).
8. Caceres, D., Vergara, I. & Gonzalez, R. Microstructural characterization of mgo thin film grown by radio-frequency sputtering, target and substrate-temperature effect. *J. Appl. Phys.* **93**, 4300 (2003).
9. Bakaul, S. R. *et al.* Single crystal functional oxides on silicon. *Nat. Commun.* **7**, 10547 (2016).
10. Hirai, T., Teramoto, K., Nagashima, K., Koike, H. & Tarui, Y. T. Y. Characterization of metal/ferroelectric/insulator/semiconductor structure with ceo₂ buffer layer. *Jpn. J. Appl. Phys.* **34**, 4163 (1995).
11. Wetzels, C., Amano, H. & Akasaki, I. Piezoelectric polarization in gainn/gan heterostructures and some consequences for device design. *Jpn. J. Appl. Phys.* **39**, 2425 (2000).
12. Wakabayashi, Y. K. *et al.* Electronic structure and magnetic properties of magnetically dead layers in epitaxial cfe₂o₄/al₂o₃/si(111) films studied by x-ray magnetic circular dichroism. *Phys. Rev. B* **96**, 104410 (2017).
13. Palneedi, H. *et al.* Laser irradiation of metal oxide films and nanostructures: Applications and advances. *Adv. Mater.* **30**, 1705148 (2018).
14. Ishibe, T. *et al.* Resistive switching memory performance in oxide hetero-nanocrystals with well-controlled interfaces. *Sci. Technol. Adv. Mater.* **21**, 195 (2020).
15. Hubbard, K. J. & Schlom, D. G. Thermodynamics stability of binary oxides in contact with silicon. *J. Mater. Res.* **11**, 2757 (1996).
16. Kaneko, S. *et al.* Crystal orientation of epitaxial oxide film on silicon substrate. *Appl. Surf. Sci.* **586**, 152776 (2022).
17. Kaneko, S. *et al.* Layer-by-layer growth of graphene on insulator in co₂ oxidizing environment. *ACS Omega* **2**, 1523 (2017).

18. Kaneko, S. *et al.* Carbon clusters on substrate surface for graphene growth - theoretical and experimental approach. *Sci. Rep.* **12**, 15809 (2022).
19. Kaneko, Y., Mikoshiba, N. & Yamashita, T. Preparation of mgo thin films by rf magnetron sputtering. *Jpn. J. Appl. Phys.* **30**, 1091 (1991).
20. Misaki, Y., Mikawa, M., Ishiguro, T. & Hamasaki, K. Effect of n₂ partial pressure on the structure of mgo thin films deposited by radio frequency-magnetron sputtering with single-crystal mgo target. *J. Vac. Sci. Tech. A* **15**, 48 (1997).
21. Senzaki, J. *et al.* Characterization of pb(zr, ti)o₃ thin films on si substrates using mgo intermediate layer for metal/ferroelectric/insulator/semiconductor field effect transistor devices. *Jpn. J. Appl. Phys.* **37**, 5150 (1998).
22. Niu, F., Hoerman, B. H. & Wessels, B. W. Epitaxial thin films of mgo on si using metalorganic molecular beam epitaxy. *J. Vac. Sci. Tech. B* **18**, 2146 (2000).
23. Caceres, D., Colera, I., Vergara, I., Gonzalez, R. & Roman, E. Characterization of mgo thin films grown by rf-sputtering. *Vacuum* **67**, 577 (2002).
24. Yamada, T., Wakiya, N., Shinozaki, K. & Mizutani, N. Growth behavior of epitaxial mgo films on si(001) by pulsed laser deposition. *Key Eng. Mater.* **253**, 119 (2003).
25. Chen, T. L., Li, X. M., Zhang, S. & Hang, X. Comparative study of epitaxial growth of pt and ir electrode films grown on mgo-buffered si(100) by pld. *Appl. Phys. A* **80**, 73 (2005).
26. Niu, F., Meier, A. & Wessels, B. E. Integration of mgo on si(001) using sro and srtio₃ buffer layers by molecular beam epitaxy. *J. Electroceramics* **13**, 149 (2004).
27. Ishiguro, T., Hiroshima, Y. & Inoue, T. Mgo(200) highly oriented film on si(100) synthesized by ambient-controlled pulsed kfr excimer laser deposition method. *Jpn. J. Appl. Phys.* **35**, 3537 (1996).
28. Kaneko, S. *et al.* Large constriction of lattice constant in epitaxial magnesium oxide thin film: Effect of point defects on lattice constant. *J. Appl. Phys.* **107**, 073523.1 (2010).
29. Kaneko, S. *et al.* Growth of nanocubic mgo on silicon substrate by pulsed laser deposition. *Jpn. J. Appl. Phys.* **52**, 01AN02 (2013).
30. Björkman, T. Cif2cell: Generating geometries for electronic structure programs. *Comput. Phys. Comm.* **182**, 1183 (2011).
31. Gonze, X. *et al.* Fsr-principle computation of material project: The abinit software project. *Comput. Mater. Sci.* **25**, 478 (2002).
32. Jollet, F., Torrent, M. & Holzwarth, N. Generation of projector augmented-wave atomic data: A 71 element validated table in the xml format. *Comput. Phys. Commun.* **185**, 1246 (2014).
33. Kaneko, S. *et al.* Superconducting transition temperatures and structure of mbe-grown nb/pd multilayers. *Phys. Rev. B* **58**, 8229 (1998).
34. Krebs, H.-U. *et al.* Pulsed laser deposition (pld): A versatile thin film technique. *Adv. in Solid State Phys.* **43**, 505 (2003).
35. Kaneko, S. *et al.* Modulation derived satellite peaks in x-ray reciprocal mapping on bismuth cuprate superconductor film. *Appl. Phys. Lett.* **85**, 2301 (2004).
36. Kaneko, S., Akiyama, K., Funakubo, H. & Yoshimoto, M. Strain-amplified structural modulation in bi-cuprate high tc superconductor. *Phys. Rev. B* **74**, 054503 (2006).
37. Kaneko, S. *et al.* Optimizing coverage of metal oxide nanoparticle prepared by pulsed laser deposition on nonenzymatic glucose detection. *Talanta* **84**, 579 (2011).
38. Dikovska, A. O., Alexandrov, M. T. & Atanasova, G. B. Silver nanoparticles produced by pld in vacuum: Role of the laser wavelength used. *Appl. Phys. A* **113**, 83 (2013).
39. Kaneko, S., Shimizu, Y. & Ohya, S. Preparation of bisrcauo multilayers by use of slower q-switched 266 nm yag laser. *Jpn. J. Appl. Phys.* **40**, 4870 (2001).
40. Narayan, J. & Larson, B. C. Domain epitaxy: A unified paradigm for thin growth. *J. Appl. Phys.* **93**, 278 (2003).
41. Estandia, S., Dix, N., Chisholm, M. F., Fina, I. & Sanchez, F. Domain-matching epitaxy of ferroelectric hfo₂sr_{0.5}o₂(111) on la_{2/3}sr_{1/3}mno₃(001). *Cryst. Growth Des.* **20**, 3801 (2020).
42. Zheleva, T., Jagannadham, K. & Narayan, J. Epitaxial growth in large-lattice-mismatch systems. *J. Appl. Phys.* **75**, 860 (1994).
43. Kim, S. & Hishita, S. Growing batio₃ thin films on si(100) with mgo-buffer layers by sputtering. *Thin Solid Films* **281–282**, 449 (1996).
44. Kim, S. & Hishita, S. Preparation and characterization of batio₃ thin films on mgo-buffered si(100) substrates by rf sputtering. *J. Mater. Res.* **12**, 1152 (1997).
45. Cáceres, D., Vergara, I. & González, R. Microstructural characterization of mgo thin films grown by radio-frequency sputtering target and substrate-temperature effect. *J. Appl. Phys.* **93**, 4300 (2003).

Acknowledgements

This study was supported in part by the Amada foundation under contract no. AF-2020227-B3 and the Collaborative Research Project of the Institute of Fluid Science, Tohoku University. Special acknowledgment to the National Cheng Kung University 90 and beyond (NCKU'90).

Author contributions

S.K. Conducted the film deposition and wrote main manuscript text, S.Y. and T.T. conducted the molecular dynamics calculation. M.A. supported DFT calculation. M.Y., M.K. and D.S. prepared oxide samples. S.S., K.S. and M.Y. provided the concept of study and prepared the draft text. M.C. and R.S.Y. setup and visualized crystal structure. A.M. and M.Y. prepared the annealed substrates and verified the surface.

Competing interests

The authors declare no competing interests.

Additional information

Correspondence and requests for materials should be addressed to S.K.

Reprints and permissions information is available at www.nature.com/reprints.

Publisher's note Springer Nature remains neutral with regard to jurisdictional claims in published maps and institutional affiliations.



Open Access This article is licensed under a Creative Commons Attribution 4.0 International License, which permits use, sharing, adaptation, distribution and reproduction in any medium or format, as long as you give appropriate credit to the original author(s) and the source, provide a link to the Creative Commons licence, and indicate if changes were made. The images or other third party material in this article are included in the article's Creative Commons licence, unless indicated otherwise in a credit line to the material. If material is not included in the article's Creative Commons licence and your intended use is not permitted by statutory regulation or exceeds the permitted use, you will need to obtain permission directly from the copyright holder. To view a copy of this licence, visit <http://creativecommons.org/licenses/by/4.0/>.

© The Author(s) 2024